European Journal of Nuclear Medicine and Molecular Imaging (2022) 49:3964–3972
https://doi.org/10.1007/s00259-022-05887-6

EDITORIAL

[^{64}Cu]Cu-ATSM: an emerging theranostic agent for cancer and neuroinflammation

Fang Xie[1] · **Weijun Wei**[2]

Published online: 3 August 2022

In the current issue of the *European Journal of Nuclear Medicine and Molecular Imaging (EJNMMI)*, Yoo et al. [1] reported that [^{64}Cu][Cu(ATSM-FITC)] positron emission tomography (PET) could accurately detect hydrogen sulfide (H_2S) in brain pathophysiology, opening a new horizon for detecting neuroinflammation by mapping H_2S level. In the below paragraphs, we first would like to introduce several targets and associated tracers used for detecting neuroinflammation and then the theranostic potential of [^{64}Cu]Cu-ATSM in preclinical and clinical settings. At the end of the manuscript, we will highlight the findings and potential applications of [^{64}Cu][Cu(ATSM-FITC)] reported by Yoo et al. By introducing the background and the most recent proceedings, readers may get a balanced understanding of the relevant information.

Brief introduction of neuroinflammation and associated tracers

Neuroinflammation is a key biological process in response to cell infection or injury that involves all the cells present within the central nervous system (CNS), including microglia, astrocytes, neurons, and macroglia [2–4]. Neuroinflammation often refers to the activation of the neuroimmune cells microglia and astrocytes. These glia cells provided pro-inflammatory and anti-inflammatory functionality and are involved in neurodegeneration, such as Alzheimer's disease (AD), Parkinson's disease (PD), and multiple sclerosis (MS), and psychiatric disorders, such as major depression disorder (MDD), schizophrenia and psychosis, and substance use. PET can visualize, characterize, and measure neuroinflammation in the brain by targeting different biomarkers from macrophages to angiogenesis [5].

The most common neuroinflammatory target is the 18 kDa translocator protein (TSPO), formerly known as peripheral benzodiazepine receptor (PBR) [6–8]. Several radiotracers were developed to quantify TSPO expression, such as the first-generation R-[^{11}C]PK11195. However, R-[^{11}C]PK11195 displayed low specific binding [9, 10]. Two second-generation tracers ([^{18}F]DPA-714 and [^{11}C]PBR28) showed about 1.5- and 5-folds higher affinity than R-[^{11}C]PK11195 [11]. [^{18}F]GE-180 is a so-called third-generation TSPO tracer with an even higher binding affinity, which provides a higher target-to-background ratio compared to these tracers [12–14]. With the development of these tracers, we can measure both activated microglia and astroglia reflecting by TSPO in AD, MS, and even depression.

There is increased TSPO expression in the frontotemporal cortex and slightly higher in the neocortex of patients with AD compared to that in healthy controls [4]. More recently, microglial activation was observed to propagate in Braak stages jointly as tau pathology by the [^{11}C]PBR28 PET study [15]. Most PET studies also indicated elevated TSPO binding in the anterior cingulate cortex or prefrontal cortex in participants with major depressive disorders [3]. MS is the most common neuroinflammatory disease which caused nontraumatic disability. As shown in Fig. 1, MS displayed increased TSPO expression in white matter lesions identified with magnetic resonance imaging (MRI); it was observed in both relapsing–remitting MS and secondary progressive MS [12, 16–18]. These TSPO binding patterns in white matter lesions are indistinguishable on MRI, which suggests that TSPO PET can detect pathophysiological heterogeneity of MS to which MRI is not sensitive or specific [4]. Furthermore, non-lesional white matter and gray matter in patients

This article is part of the Topical Collection on Oncology - General

✉ Weijun Wei
wwei@shsmu.edu.cn

[1] PET Center, Huashan Hospital, Fudan University, Shanghai 200040, China

[2] Department of Nuclear Medicine, Institute of Clinical Nuclear Medicine, School of Medicine, Renji Hospital, Shanghai Jiao Tong University, Shanghai 200127, China

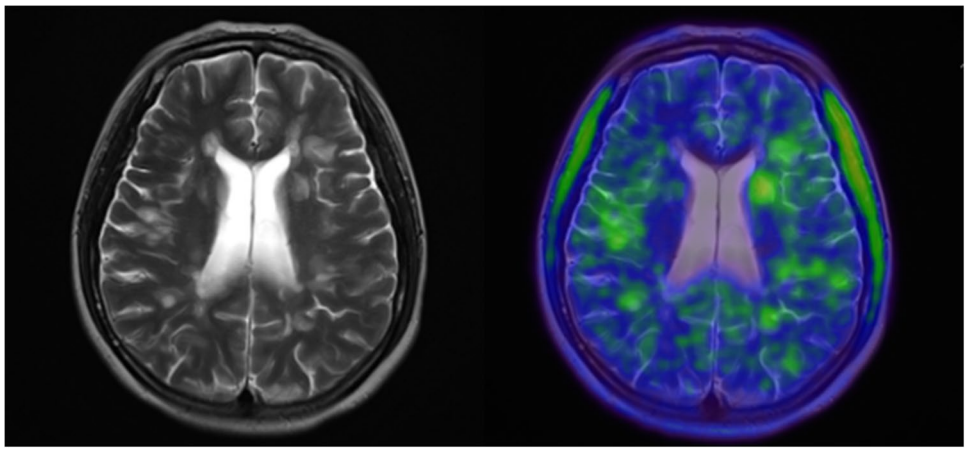

Fig. 1 Representative [^{18}F] DPA-714 PET in a 28-year-old female patient with MS. T2-weighted MR (left) and TSPO PET (right) images were provided by the PET center, Huashan Hospital

with MS also showed greater TSPO binding than that in age-matched healthy controls.

But there were several limitations for TSPO as a biomarker of neuroinflammation. Firstly, the expression of TSPO by astrocytes and in the vascular endothelium was not neglected other than its expression in the brain by microglia. Secondly, TSPO PET is sensitive to polymorphism (rs6971) in the TSPO gene, which generated high-affinity binders (two copies of the major allele), mixed-affinity binders (heterozygous allele), and low-affinity binders (two copies of the rare allele). It means different PET signals could be produced by individuals with the same TSPO density but different genotypes. Thirdly, the lack of a true reference region requires kinetic modeling through the use of the metabolite-corrected arterial input function for accurate measurement of its density. These shortcomings limited the application of TSPO PET, especially the quantification of TSPO. More importantly, TSPO PET was found to reflect the density of inflammatory cells rather than their activation in humans, because its expression in human myeloid cells is related to different phenomena. Therefore, TSPO PET can reflect activated microglia in rodents but not in humans, which means the interpretation of TSPO PET data requires revision [19]. Therefore, more neuroimmune imaging biomarkers are necessary to overcome the limitation of TSPO PET. Novel inflammatory targets, including P2X7, P2Y12, colony-stimulating factor 1 receptor (CSF1R), monoamine oxidase B (MAO-B), cyclooxygenase isoenzymes COX-1, and COX-2, were validated in human diseases.

Purinergic receptors were classified as P1 and P2 receptors. P2 receptors are further subdivided into P2X and P2Y receptors; seven P2X receptors and eight P2Y receptors were identified. Among them, P2X7 and P2Y12 are the most promising targets for imaging neuroinflammation. The P2X7 receptor is expressed on immune cells such as monocytes, macrophages, and microglia. However, the P2Y12 receptor is only expressed on microglia but not on peripheral macrophages in the brain [20]. Some P2X7 tracers were developed and evaluated in humans, such as [^{11}C] GSK1482160, [^{11}C]JNJ-54173717, and [^{18}F]JNJ-64413739. Although P2X7 PET displayed excellent results in MS, the application in other diseases is still not successful. P2X7 PET demonstrated no difference between amyotrophic lateral sclerosis (ALS) and controls and between PD and controls [21, 22]. For the P2Y12 receptor, several radiotracers were developed, but currently, no tracer can cross the blood–brain barrier (BBB) [23]. Therefore, the development of the brain penetrating P2Y12R PET tracer is still urgent.

CSF1R is another promising neuroinflammatory biomarker which predominantly expressed by microglia in the CNS. Its expression in other cells, such as neurons, is limited. It was also reported to involve in neurodegeneration and psychiatric disorders. CSF1R was used as a therapeutic target in various autoimmune disorders and cancers. Mutations in the CSF1R gene causing an autosomal dominant disease of hereditary diffuse leukoencephalopathy with spheroids (HDLS) also emphasized its significance [24, 25]. However, suitable CSF1R radiotracers are not available now. [^{11}C]CPPC and [^{11}C]GW2580 are the most promising ones investigated in inflammatory animal models [26, 27]. An autoradiography study also confirmed the increased (75–99%) radiotracer binding in the AD brain by [^{11}C]CPPC [27]. The major issue of [^{11}C]CPPC is that the sensitivity is not adequate to detect the low density of CSF1R in the healthy brain.

MAO-B is located both in neurons and astrocytes and overexpressed under pathological conditions associated with astrocytosis. MAO-B is considered a good biomarker of astrocytes and displayed a significant role in the treatment and diagnosis of neurodegenerative and other brain disorders [28]. PET imaging of MAO-B could provide opportunities for the quantification of astrocytosis. The first generation of MAO-B tracer of L-[^{11}C]deprenyl was originally developed in the 1980s [29]. Recently, a novel MAO-B tracer, [^{18}F] SMBT-1, was developed from the tau tracer, [^{18}F]THK-5351 [30, 31]. [^{18}F]SMBT-1 displayed high binding affinity and

selectivity to MAO-B and reversible kinetics. It is also valuable to measure astrocytosis in AD patients.

COX is essential in the synthesis process of pro-inflammatory prostanoids, and their release as inflammatory mediators is significant to neuroinflammation. COX-1 is mainly localized in microglia, contributing to pro-inflammatory responses, while COX-2 is also expressed in neurons. COX-2 is quickly and dramatically upregulated by inflammation. Therefore, COXs were used as the biomarkers for the treatment and diagnosis of chronic inflammatory diseases, such as pain, fever, arthritis, and neurodegeneration. Two selective tracers were validated in human volunteers, [^{11}C]PS13 for COX-1 and [^{11}C]MC1 for COX-2. [^{11}C]PS13 displayed the highest uptake in the hippocampus and occipital cortex, followed by the pericentral cortex and adjacent neocortices in the brain [32]. Physiological COX-1 expression in these regions was confirmed by COX-1 mRNA expression in the healthy human brain. [^{11}C]MC1 was investigated in patients with rheumatoid arthritis, and increased binding in the affected joints was observed. [^{11}C]MC1 also found no detectable binding in the brain of healthy volunteers. However, patients with rheumatoid arthritis displayed elevated brain uptake, in an order of neocortex, subcortical gray matter, and cerebellum [33]. The ability of [^{11}C]MC1 in the measurement of COX-2 expression was also validated in the rhesus monkey brain and periphery after lipopolysaccharide injection [33].

Although tremendous targets were investigated as neuroinflammatory biomarkers, most of them targeted glia cells. The shortcomings of these targets and associated tracers also limited their applications. Therefore, discovery of new targets and development of new tracers are also necessary. Although traditionally known as a toxic gas, accumulating evidence supports that hydrogen sulfide (H_2S) plays important roles in CNS diseases and traumatic brain injury [34–37]. Measurement of H_2S levels in the brain could be a new strategy to monitor the CNS diseases.

Cu-ATSM in imaging cancers and neurodegenerative diseases

The copper II glyoxal bis(4-methyl-3-thiosemicarbazone) (Cu(II)-GTSM) (Fig. 2a) can deliver exogenously bound Cu directly into cells and activate pathways where Cu is a key cofactor. Copper II diacetyl-bis(4-methyl-3-thiosemicarbazone) (Cu(II)-ATSM) (Fig. 2b) is a biosimilar and only releases the exogenously bound Cu under hypoxic conditions. Both Cu-ATSM and ATSM are quickly cleared from the circulation with corresponding half-lives ($T_{1/2}$) of 21.5 and 22.4 min, respectively [38]. The BBB is a highly selective gateway regulating the influx and efflux of molecules from the systemic circulation into the brain and in the reverse direction. Cu(II)-ATSM has enhanced permeability and can penetrate the BBB [39].

Both the properties and species of Cu affect the cellular uptake [40, 41]. Although the full mechanisms underlying the uptake of Cu-ATSM remain to be elucidated, the proposed mechanisms are shown in Fig. 3. One potential mechanism is the penetration of Cu(II)-ATSM into mitochondria and reduction of Cu(II) to Cu(I), leading to irreversible retention of metal or radiometal in the hypoxic cells [42, 43]. More recently, Yoshii et al. found that uptake of Cu-ATSM not only reflects hypoxia but also indicates the over-reduced intracellular states caused by mitochondrial dysfunction [44]. In normoxic cells, the Cu(I)-ATSM compound is

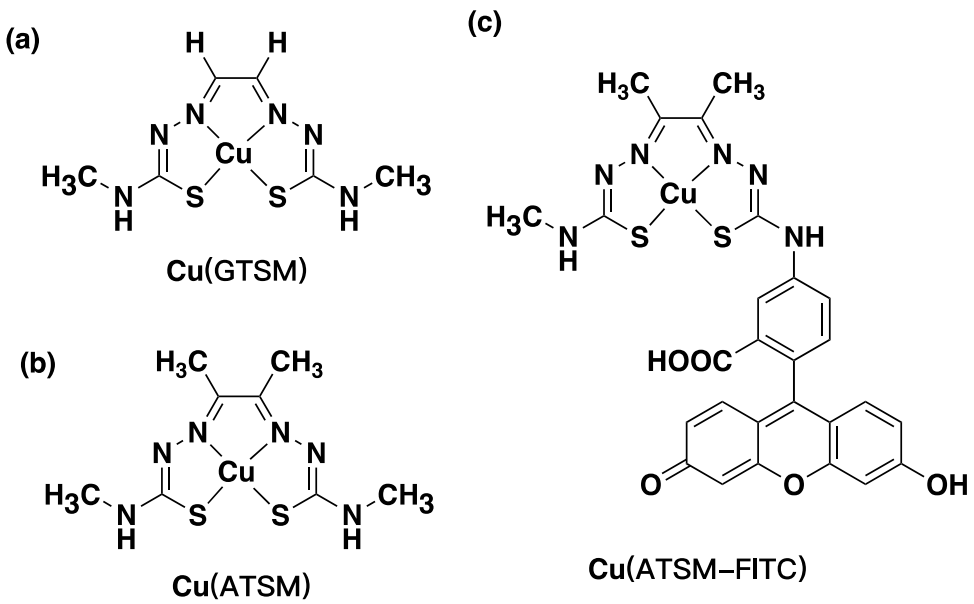

Fig. 2 Chemical structures of **a** Cu(GTSM), **b** Cu(ATSM), and **c** Cu(ATSM-FITC)

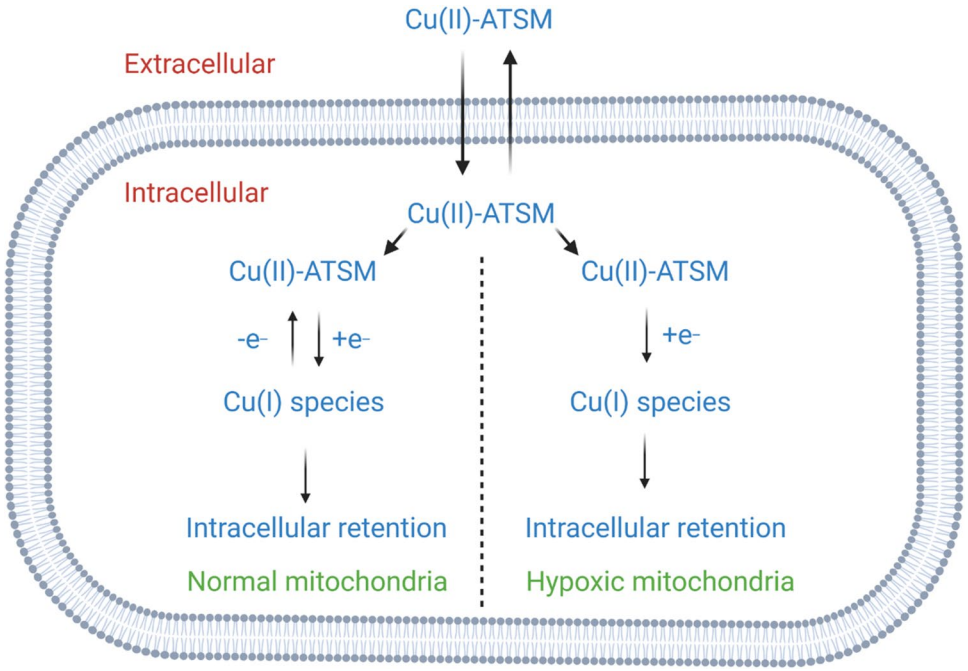

Fig. 3 Mechanisms mediating cellular uptake of retention of Cu-ATSM under normal and hypoxic conditions. Cu(II)-ATSM readily penetrates cells due to its low molecular weight, high membrane permeability, and low redox potential. In over-reduced cells such as when cells are under hypoxic conditions, the Cu(II) in Cu(II)-ATSM is reduced to Cu(I), which is released from the ATSM and trapped inside the cells. Another recently proposed mechanism accounting for the deposition of the tracers is the formation and deposition of CuS when there is an increased level of H_2S in the CNS [1]

rapidly re-oxidized into Cu(II)-ATSM by molecular oxygen and washed out from the cells [45, 46]. Another potential mechanism is the disassociation of Cu(II) from copper(II) complexes and the reduction of Cu(II) to Cu(I) by reductases in the circulation or tumor microenvironment. Hypoxic tumor cells have increased expression of copper transporter 1 (CTR-1) which mediates the transportation of Cu(I) into tumor cells [47].

When labeled with Cu isotopes (^{60}Cu [half-life, 0.395 h; β^+-decay, 92.5%; electron capture, 7.5%], ^{62}Cu [half-life, 0.16 h; β^+-decay, 98%; electron capture, 2%], and ^{64}Cu [half-life, 12.7 h; β^+-decay, 17.4%; β^--decay, 38.5%; electron capture, 43%]), they can be used for tumor hypoxia imaging and blood perfusion visualization. In 1996, Fujibayashi et al. reported that [^{62}Cu]Cu-ATSM had high brain and heart uptake but was quickly washed out from these tissues. Moreover, [^{62}Cu]Cu-ATSM had significantly increased heart uptake under hypoxic conditions [48]. This was followed by a translational study in 2000 reporting the safety profiles, rapid clearance from circulation, and accumulation of the tracer in the tumors within minutes [49]. Meanwhile, Lewis et al. elucidated that uptake of Cu-ATSM was dependent on tissue oxygen pressure and thus validated the value in imaging hypoxia [50, 51]. In non-small cell lung cancers (NSCLCs), the uptake patterns of [^{62}Cu]Cu-ATSM and ^{18}F-FDG differed in squamous cell carcinoma (SCC) and adenocarcinomas [52]. Similarly, in a recent study including 30 patients with head-and-neck cancers, Okazawa and co-authors demonstrated that high accumulation of [^{62}Cu]Cu-ATSM in the periphery and intense uptake of ^{18}F-FDG in the center were seen in SCCs. In comparison, the uptake patterns of the two tracers in adenocarcinomas were homogeneous [53]. Ikawa et al. reported that PET imaging with [^{62}Cu]Cu-ATSM could visualize the regional oxidative stress in a patient with mitochondrial myopathy, encephalopathy, lactic acidosis, and stroke-like episodes (MELAS) [54]. Oxidative stress and mitochondrial dysfunction may contribute to the pathogenesis of PD. The same group then elucidated the uptake patterns of [^{62}Cu]Cu-ATSM in patients with PD, reporting a higher accumulation of [^{62}Cu]Cu-ATSM in the striata of the PD patients than that in the controls [55]. In patients with cerebrovascular disease, the information of dynamic [^{62}Cu]Cu-ATSM correlated well with that of ^{15}O tracers in assessing cerebral blood flow and oxygen extraction fraction [56]. [^{62}Cu]Cu-ATSM uptake was significantly higher in grade IV than in grade III gliomas and correlated well with HIF-1α expression [57]. In addition to probing hypoxia, Dehdashti et al. further reported that the tumor-to-muscle activity ratio of [^{60}Cu]Cu-ATSM could predict the treatment responsiveness in NSCLCs and cervical cancers [58, 59].

Compared to ^{60}Cu or ^{62}Cu-labeled agents, ^{64}Cu-labeled agents are longer-lived radiopharmaceuticals that will facilitate shipping to multiple centers for multi-center clinical trials. In particular, β^- decay (38.5%) and Auger electron emission of ^{64}Cu open the possibility of therapeutic applications with [^{64}Cu]Cu-ATSM under proper conditions [60, 61]. [^{64}Cu]Cu-ATSM largely accumulated around the outer rim of tumor masses where hypoxic but active tumor cells resided [62]. Granted as an Investigational New Drug by the US Food and Drug Administration, a head-to-head comparison of [^{60}Cu]Cu-ATSM and [^{64}Cu]Cu-ATSM showed

a significant uptake correlation of the two tracers in 10 patients with uterine cervical cancers. It is notable that [^{64}Cu]Cu-ATSM PET images had better tumor-to-background ratios than that of [^{60}Cu]Cu-ATSM [63]. Moreover, among several radiotracers for imaging tumor hypoxia, [^{64}Cu]Cu-ATSM has potential advantages over others in several aspects. [^{64}Cu]Cu-ATSM may have enhanced BBB penetration over [^{18}F]FAZA which is cleared from the urinary system [64, 65]. [^{64}Cu]Cu-ATSM had higher uptake in the hypoxia tissues and more rapid washout in normoxic cells than [^{18}F]fluoromisonidazole ([^{18}F]FMISO), the latter requiring at least 2-h equilibrium before scanning is commenced [39, 45, 66]. However, Little et al. found that [^{18}F]FMISO but not [^{64}Cu]Cu-ATSM or [^{64}Cu]Cu-ATSE identified hypoxic regions in acute ischemic stroke models [66], validating the negative results previously reported [67]. So far, nitroimidazole-derived tracers, such as [^{18}F]FMISO and the sugar-coupled tracer [^{18}F]FAZA, are still the prime contenders in imaging hypoxia [68].

[^{64}Cu]Cu-ATSM is currently in clinical trials for imaging tumor hypoxia in locally advanced rectum cancer (NCT03951337) and bulky tumors (NCT04875871). Automated cyclotron production and synthesis of [^{64}Cu]Cu-ATSM with a commercially available synthesis module (GE Tracerlab™ FX2 N) has been reported by Liu et al. [69]. Multiple administration of [^{64}Cu]Cu-ATSM may result in liver toxicity [70, 71]. Administration of penicillamine, a heavy metal chelator, could reduce radiation absorption doses in critical organs such as the liver and small intestine [72]. Different formulations of [^{64}Cu]Cu-ATSM have been developed and validated by two research groups for diagnostic and theranostic applications, respectively [38, 63]. The potential risk associated with the chemical impurities from [^{64}Cu]Cu-ATSM degradation is negligible, even in a therapeutic dose of [^{64}Cu]Cu-ATSM [73]. PET imaging with [^{64}Cu]Cu-ATSM may provide clinically relevant information about tumor oxygenation (hypoxia) and value in predicting therapeutic responses and survival in patients with solid tumors [74]. While most of the clinical trials are planned to image tumor hypoxia and predict the therapeutic responses of [^{64}Cu]Cu-ATSM, there are also clinical studies evaluating the safety profiles and preliminary efficacies of Cu(II)ATSM in patients with PD or amyotrophic lateral sclerosis/motor neuron disease. The information on several finished and ongoing clinical trials is summarized in Table 1. Meanwhile, [^{64}Cu]Cu-ATSM is fully exploited as a theranostic agent in Japan. Therefore, uncovering mechanisms other than the well-recognized radiobiological effects may help understand the therapeutic effects [75, 76].

[^{64}Cu]Cu-ATSM-FITC is an emerging agent sensing hydrogen sulfide

As mentioned above, accumulating evidence indicates that H_2S plays important roles in the pathogenesis of a range of brain tissues [77]. A recent study elucidated that Cu(II)-ATSM, but not Cu(II)-GTSM, enhanced P-glycoprotein (P-gp) expression and may further contribute to the clearance of amyloid beta (Aβ) from the brain [78]. How to noninvasively and reliably detect endogenous level H_2S remains a challenge. In the long run to develop probes for sensing H_2S levels, both radioactive and non-radioactive probes have been developed [79]. Radioactive probes have advantages over fluorescent probes in terms of detection sensitivity, penetration ability, and high consistency. In the recent work published in the *EJNMMI* [1], Yoo et al. exquisitely developed [^{64}Cu]Cu-ATSM-FITC (Fig. 2c) based on the bis(thiosemicarbazone) backbone. The tracer penetrated BBB and accumulated exceptionally (> 9%ID/g) high in the mice brain, due to the lipophilicity of the radiotracer with a $D_{7.4}$ value of ~ 1.70. [^{64}Cu]Cu-ATSM-FITC reacts with H_2S instantly to immobilize gaseous H_2S into an insoluble copper sulfide ([^{64}Cu]CuS) precipitate. While [^{64}Cu]Cu-ATSM-FITC has no fluorescence signal due

Table 1 Registered clinical trials using [^{64}Cu]Cu-ATSM or Cu(II)ATSM

Tracer/agent	Cancer types	Application purposes	Status	Registration number
[^{64}Cu]Cu-ATSM	Rectum cancer	Predict response of neoadjuvant therapies	Ongoing	NCT03951337
[^{64}Cu]Cu-ATSM	Bulky tumors (≥ 6 cm)	Imaging of tumor hypoxia	Ongoing	NCT04875871
[^{61}Cu]Cu-ATSM	Solid tumors	Imaging of tumor hypoxia	Terminated	NCT00585117
[^{64}Cu]Cu-ATSM	Glioblastoma	Predict response of radiotherapy and chemotherapy	Terminated	NCT02329795
[^{64}Cu]Cu-ATSM	Cervical cancer	Predict chemoradiotherapy response and progression-free survival	Terminated	NCT00794339
[^{64}Cu]Cu-ATSM	Non-small cell lung cancer	Imaging of tumor hypoxia and predicting chemotherapy response	Withdrawn	NCT01006226
Cu(II)ATSM	Parkinson's disease	Confirm tolerability and assess preliminary efficacy	Completed	NCT03204929
Cu(II)ATSM	Amyotrophic lateral sclerosis/motor neuron disease	Dose acceleration and preliminary efficacy evaluation	Completed	NCT02870634

to fluorescence quenching by Cu(II), the released ATSM-FITC ligand emits fluorescence. Elegant in vitro cell studies and in vivo PET imaging studies validated that uptake of [^{64}Cu]Cu-ATSM-FITC was H_2S-dependent. Furthermore, the authors reported that [^{64}Cu]Cu-ATSM-FITC had higher uptake in lipopolysaccharide-induced neuroinflammation models.

The preclinical promise can potentially be translated into clinical reality to detect brain diseases [80–83]. Initial studies have shown the diffuse uptake of [^{62}Cu]Cu-ATSM in healthy controls and neurological diseases [54, 55]. Since [^{64}Cu]Cu-ATSM can delineate ischemic and hypoxic changes [84] as well as over-reduced intracellular states caused by mitochondrial dysfunction [44, 54], the net signal of [^{64}Cu]Cu-ATSM or [^{64}Cu]Cu-ATSM-FITC contributed by H_2S should be carefully interpreted. Sequential use of [^{64}Cu]Cu-ATSM (or [^{64}Cu]Cu-ATSM-FITC) and tracers reflecting hypoxia or blood flow may better address clinical challenges. Furthermore, the role of CTR-1 in mediating the uptake of ^{64}Cu-labeled radioligands should be carefully examined. From a diagnostic perspective, understanding mechanisms accounting for [^{64}Cu]Cu-ATSM uptake is essential to fully interpret the imaging findings and find the application scenarios. Visualization of H_2S levels in neurological diseases is attractive. As the authors mentioned, [^{64}Cu]Cu-ATSM-FITC may help diagnose various diseases such as traumatic brain injury, stroke, encephalitis, and neurodegenerative diseases (e.g., PD and AD) [1]. Besides that, [^{64}Cu]Cu-ATSM-FITC and other similar probes can also be used to detect cardiovascular diseases such as myocardium infarct and atherosclerosis [79, 85]. Further translation studies are needed to fill the gaps and address the clinical value.

Author contribution W. Wei and F. Xie contributed equally to the work.

Funding This research was funded by the National Key Research and Development Program of China (Grant No. 2020YFA0909000), the National Natural Science Foundation of China (Grant No. 82001878), and the Shanghai Rising-Star Program (Grant No. 20QA1406100).

Declarations

Ethics approval Institutional Review Board approval was not required because the paper is an Editorial.

Consent to participate Not applicable.

Conflict of interest The authors declare no competing interests.

References

1. Nam B, Lee W, Sarkar S, Kim JH, Bhise A, Park H, et al. In vivo detection of hydrogen sulfide in the brain of live mouse: application in neuroinflammation models. Eur J Nucl Med Mol Imaging. 2022. https://doi.org/10.1007/s00259-022-05854-1.
2. Jain P, Chaney AM, Carlson ML, Jackson IM, Rao A, James ML. Neuroinflammation PET imaging: current opinion and future directions. J Nucl Med : Off Publ Soc Nucl Med. 2020;61:1107–12. https://doi.org/10.2967/jnumed.119.229443.
3. Meyer JH, Cervenka S, Kim M-J, Kreisl WC, Henter ID, Innis RB. Neuroinflammation in psychiatric disorders: PET imaging and promising new targets. Lancet Psychiat. 2020;7:1064–74. https://doi.org/10.1016/s2215-0366(20)30255-8.
4. Kreisl WC, Kim M-J, Coughlin JM, Henter ID, Owen DR, Innis RB. PET imaging of neuroinflammation in neurological disorders. Lancet Neurol. 2020;19:940–50. https://doi.org/10.1016/s1474-4422(20)30346-x.
5. Wu C, Li F, Niu G, Chen X. PET imaging of inflammation biomarkers. Theranostics. 2013;3:448–66. https://doi.org/10.7150/thno.6592.
6. Zhang L, Hu K, Shao T, Hou L, Zhang S, Ye W, et al. Recent developments on PET radiotracers for TSPO and their applications in neuroimaging. Acta Pharm Sin B. 2021;11:373–93. https://doi.org/10.1016/j.apsb.2020.08.006.
7. Tai YF, Pavese N, Gerhard A, Tabrizi SJ, Barker RA, Brooks DJ, et al. Imaging microglial activation in Huntington's disease. Brain Res Bull. 2007;72:148–51. https://doi.org/10.1016/j.brainresbull.2006.10.029.
8. Weissman BA, Raveh L. Peripheral benzodiazepine receptors: on mice and human brain imaging. J Neurochem. 2003;84:432–7. https://doi.org/10.1046/j.1471-4159.2003.01568.x.
9. Bartels AL, Willemsen AT, Doorduin J, de Vries EF, Dierckx RA, Leenders KL. [11C]-PK11195 PET: quantification of neuroinflammation and a monitor of anti-inflammatory treatment in Parkinson's disease? Parkinsonism Relat Disord. 2010;16:57–9. https://doi.org/10.1016/j.parkreldis.2009.05.005.
10. Venneti S, Lopresti BJ, Wang G, Hamilton RL, Mathis CA, Klunk WE, et al. PK11195 labels activated microglia in Alzheimer's disease and in vivo in a mouse model using PET. Neurobiol Aging. 2009;30:1217–26. https://doi.org/10.1016/j.neurobiolaging.2007.11.005.
11. Schubert J, Tonietto M, Turkheimer F, Zanotti-Fregonara P, Veronese M. Supervised clustering for TSPO PET imaging. Eur J Nucl Med Mol Imaging. 2021;49:257–68. https://doi.org/10.1007/s00259-021-05309-z.
12. Unterrainer M, Mahler C, Vomacka L, Lindner S, Havla J, Brendel M, et al. TSPO PET with [(18)F]GE-180 sensitively detects focal neuroinflammation in patients with relapsing-remitting multiple sclerosis. Eur J Nucl Med Mol Imaging. 2018;45:1423–31. https://doi.org/10.1007/s00259-018-3974-7.
13. Vomacka L, Albert NL, Lindner S, Unterrainer M, Mahler C, Brendel M, et al. TSPO imaging using the novel PET ligand [(18)F]GE-180: quantification approaches in patients with multiple sclerosis. EJNMMI Res. 2017;7:89. https://doi.org/10.1186/s13550-017-0340-x.
14. Albert NL, Unterrainer M, Fleischmann DF, Lindner S, Vettermann F, Brunegraf A, et al. TSPO PET for glioma imaging using the novel ligand (18)F-GE-180: first results in patients with glioblastoma. Eur J Nucl Med Mol Imaging. 2017;44:2230–8. https://doi.org/10.1007/s00259-017-3799-9.
15. Pascoal TA, Benedet AL, Ashton NJ, Kang MS, Therriault J, Chamoun M, et al. Microglial activation and tau propagate jointly across Braak stages. Nat Med. 2021;27:1592–9. https://doi.org/10.1038/s41591-021-01456-w.
16. Plastini MJ, Desu HL, Brambilla R. Dynamic responses of microglia in animal models of multiple sclerosis. Front Cell Neurosci. 2020;14:269. https://doi.org/10.3389/fncel.2020.00269.
17. Sucksdorff M, Matilainen M, Tuisku J, Polvinen E, Vuorimaa A, Rokka J, et al. Brain TSPO-PET predicts later disease progression

independent of relapses in multiple sclerosis. Brain : J Neurol. 2020;143:3318–30. https://doi.org/10.1093/brain/awaa275.
18. Hagens MHJ, Golla SV, Wijburg MT, Yaqub M, Heijtel D, Steenwijk MD, et al. In vivo assessment of neuroinflammation in progressive multiple sclerosis: a proof of concept study with [(18)F] DPA714 PET. J Neuroinflammation. 2018;15:314. https://doi.org/10.1186/s12974-018-1352-9.
19. Nutma E, Fancy N, Marzin M, Tsartsalis S, Muirhead RCJ, Falk I, et al. Translocator protein is a marker of activated microglia in rodent 2 models but not human neurodegenerative diseases. 2022. https://www.researchsquare.com/article/rs-1420033/v1.
20. Beaino W, Janssen B, Kooij G, van der Pol SMA, van Het Hof B, van Horssen J, et al. Purinergic receptors P2Y12R and P2X7R: potential targets for PET imaging of microglia phenotypes in multiple sclerosis. J Neuroinflammation. 2017;14:259. https://doi.org/10.1186/s12974-017-1034-z.
21. Van Weehaeghe D, Koole M, Schmidt ME, Deman S, Jacobs AH, Souche E, et al. [(11)C]JNJ54173717, a novel P2X7 receptor radioligand as marker for neuroinflammation: human biodistribution, dosimetry, brain kinetic modelling and quantification of brain P2X7 receptors in patients with Parkinson's disease and healthy volunteers. Eur J Nucl Med Mol Imaging. 2019;46:2051–64. https://doi.org/10.1007/s00259-019-04369-6.
22. Van Weehaeghe D, Van Schoor E, De Vocht J, Koole M, Attili B, Celen S, et al. TSPO versus P2X7 as a target for neuroinflammation: an in vitro and in vivo study. J Nucl Med: Off Publ Soc Nucl Med. 2020;61:604–7. https://doi.org/10.2967/jnumed.119.231985.
23. van der Wildt B, Janssen B, Pekosak A, Steen EJL, Schuit RC, Kooijman EJM, et al. Novel thienopyrimidine-based PET tracers for P2Y12 receptor imaging in the brain. ACS Chem Neurosci. 2021;12:4465–74. https://doi.org/10.1021/acschemneuro.1c00641.
24. Tada M, Konno T, Tada M, Tezuka T, Miura T, Mezaki N, et al. Characteristic microglial features in patients with hereditary diffuse leukoencephalopathy with spheroids. Ann Neurol. 2016;80:554–65. https://doi.org/10.1002/ana.24754.
25. Rademakers R, Baker M, Nicholson AM, Rutherford NJ, Finch N, Soto-Ortolaza A, et al. Mutations in the colony stimulating factor 1 receptor (CSF1R) gene cause hereditary diffuse leukoencephalopathy with spheroids. Nat Genet. 2011;44:200–5. https://doi.org/10.1038/ng.1027.
26. Zhou X, Ji B, Seki C, Nagai Y, Minamimoto T, Fujinaga M, et al. PET imaging of colony-stimulating factor 1 receptor: a head-to-head comparison of a novel radioligand, (11)C-GW2580, and (11)C-CPPC, in mouse models of acute and chronic neuroinflammation and a rhesus monkey. J Cereb Blood Flow Metab : Off J Int Soc Cereb Blood Flow Metab. 2021;41:2410–22. https://doi.org/10.1177/0271678X211004146.
27. Horti AG, Naik R, Foss CA, Minn I, Misheneva V, Du Y, et al. PET imaging of microglia by targeting macrophage colony-stimulating factor 1 receptor (CSF1R). Proc Natl Acad Sci USA. 2019;116:1686–91. https://doi.org/10.1073/pnas.1812155116.
28. Liu Y, Jiang H, Qin X, Tian M, Zhang H. PET imaging of reactive astrocytes in neurological disorders. Eur J Nucl Med Mol Imaging. 2022;49:1275–87. https://doi.org/10.1007/s00259-021-05640-5.
29. Logan J, Fowler JS, Volkow ND, Wang G-J, MacGregor RR, Shea C. Reproducibility of repeated measures of deuterium substituted [11C]L-deprenyl ([11C]L-deprenyl-D2) binding in the human brain. Nucl Med Biol. 2000;27:43–9. https://doi.org/10.1016/s0969-8051(99)00088-8.
30. Villemagne VL, Harada R, Dore V, Furumoto S, Mulligan R, Kudo Y, et al. First-in-human evaluation of (18)F-SMBT-1, a novel (18)F-labeled MAO-B PET tracer for imaging reactive astrogliosis. Journal of nuclear medicine: official publication. J Nucl Med. 2022;jnumed.121.263254. https://doi.org/10.2967/jnumed.121.263254
31. Harada R, Hayakawa Y, Ezura M, Lerdsirisuk P, Du Y, Ishikawa Y, et al. (18)F-SMBT-1: a selective and reversible PET tracer for monoamine oxidase-B imaging. J Nucl Med: Off Publ Soc Nucl Med. 2021;62:253–8. https://doi.org/10.2967/jnumed.120.244400.
32. Kim MJ, Lee JH, Juarez Anaya F, Hong J, Miller W, Telu S, et al. First-in-human evaluation of [(11)C]PS13, a novel PET radioligand, to quantify cyclooxygenase-1 in the brain. Eur J Nucl Med Mol Imaging. 2020;47:3143–51. https://doi.org/10.1007/s00259-020-04855-2.
33. Shrestha S, Kim MJ, Eldridge M, Lehmann ML, Frankland M, Liow JS, et al. PET measurement of cyclooxygenase-2 using a novel radioligand: upregulation in primate neuroinflammation and first-in-human study. J Neuroinflammation. 2020;17:140. https://doi.org/10.1186/s12974-020-01804-6.
34. Zhang X, Bian J-S. Hydrogen sulfide: a neuromodulator and neuroprotectant in the central nervous system. ACS Chem Neurosci. 2014;5:876–83. https://doi.org/10.1021/cn500185g.
35. Moore PK, Bhatia M, Moochhala S. Hydrogen sulfide: from the smell of the past to the mediator of the future? Trends Pharmacol Sci. 2003;24:609–11. https://doi.org/10.1016/j.tips.2003.10.007.
36. Paul BD, Snyder SH. Gasotransmitter hydrogen sulfide signaling in neuronal health and disease. Biochem Pharmacol. 2018;149:101–9. https://doi.org/10.1016/j.bcp.2017.11.019.
37. Hu L-F, Lu M, Hon Wong PT, Bian J-S. Hydrogen sulfide: neurophysiology and neuropathology. Antioxid Redox Signal. 2010;15:405–19. https://doi.org/10.1089/ars.2010.3517.
38. Matsumoto H, Yoshii Y, Baden A, Kaneko E, Hashimoto H, Suzuki H, et al. Preclinical pharmacokinetic and safety studies of copper-diacetyl-bis(N(4)-methylthiosemicarbazone) (Cu-ATSM): translational studies for internal radiotherapy. Transl Oncol. 2019;12:1206–12. https://doi.org/10.1016/j.tranon.2019.05.017.
39. Vavere AL, Lewis JS. Cu-ATSM: a radiopharmaceutical for the PET imaging of hypoxia. Dalton Trans. 2007;(43):4893–902. https://doi.org/10.1039/b705989b.
40. Dearling JL, Packard AB. On the destiny of (copper) species. J Nucl Med. 2014;55:7–8. https://doi.org/10.2967/jnumed.113.132480.
41. Dearling JL, Packard AB. Some thoughts on the mechanism of cellular trapping of Cu(II)-ATSM. Nucl Med Biol. 2010;37:237–43. https://doi.org/10.1016/j.nucmedbio.2009.11.004.
42. Obata A, Yoshimi E, Waki A, Lewis JS, Oyama N, Welch MJ, et al. Retention mechanism of hypoxia selective nuclear imaging/radiotherapeutic agent cu-diacetyl-bis(N4-methylthiosemicarbazone) (Cu-ATSM) in tumor cells. Ann Nucl Med. 2001;15:499–504. https://doi.org/10.1007/BF02988502.
43. Holland JP, Giansiracusa JH, Bell SG, Wong LL, Dilworth JR. In vitro kinetic studies on the mechanism of oxygen-dependent cellular uptake of copper radiopharmaceuticals. Phys Med Biol. 2009;54:2103–19. https://doi.org/10.1088/0031-9155/54/7/017.
44. Yoshii Y, Yoneda M, Ikawa M, Furukawa T, Kiyono Y, Mori T, et al. Radiolabeled Cu-ATSM as a novel indicator of overreduced intracellular state due to mitochondrial dysfunction: studies with mitochondrial DNA-less rho0 cells and cybrids carrying MELAS mitochondrial DNA mutation. Nucl Med Biol. 2012;39:177–85. https://doi.org/10.1016/j.nucmedbio.2011.08.008.
45. Lewis JS, McCarthy DW, McCarthy TJ, Fujibayashi Y, Welch MJ. Evaluation of 64Cu-ATSM in vitro and in vivo in a hypoxic tumor model. J Nucl Med. 1999;40:177–83.
46. Maurer RI, Blower PJ, Dilworth JR, Reynolds CA, Zheng Y, Mullen GE. Studies on the mechanism of hypoxic selectivity in copper bis(thiosemicarbazone) radiopharmaceuticals. J Med Chem. 2002;45:1420–31. https://doi.org/10.1021/jm0104217.

47. White C, Kambe T, Fulcher YG, Sachdev SW, Bush AI, Fritsche K, et al. Copper transport into the secretory pathway is regulated by oxygen in macrophages. J Cell Sci. 2009;122:1315–21. https://doi.org/10.1242/jcs.043216.
48. Fujibayashi Y, Taniuchi H, Yonekura Y, Ohtani H, Konishi J, Yokoyama A. Copper-62-ATSM: a new hypoxia imaging agent with high membrane permeability and low redox potential. J Nucl Med. 1997;38:1155–60.
49. Takahashi N, Fujibayashi Y, Yonekura Y, Welch MJ, Waki A, Tsuchida T, et al. Evaluation of 62Cu labeled diacetyl-bis(N4-methylthiosemicarbazone) as a hypoxic tissue tracer in patients with lung cancer. Ann Nucl Med. 2000;14:323–8. https://doi.org/10.1007/BF02988690.
50. Lewis JS, Sharp TL, Laforest R, Fujibayashi Y, Welch MJ. Tumor uptake of copper-diacetyl-bis(N(4)-methylthiosemicarbazone): effect of changes in tissue oxygenation. J Nucl Med. 2001;42:655–61.
51. O'Donoghue JA, Zanzonico P, Pugachev A, Wen B, Smith-Jones P, Cai S, et al. Assessment of regional tumor hypoxia using 18F-fluoromisonidazole and 64Cu(II)-diacetyl-bis(N4-methylthiosemicarbazone) positron emission tomography: comparative study featuring microPET imaging, Po2 probe measurement, autoradiography, and fluorescent microscopy in the R3327-AT and FaDu rat tumor models. Int J Radiat Oncol Biol Phys. 2005;61:1493–502. https://doi.org/10.1016/j.ijrobp.2004.12.057.
52. Lohith TG, Kudo T, Demura Y, Umeda Y, Kiyono Y, Fujibayashi Y, et al. Pathophysiologic correlation between 62Cu-ATSM and 18F-FDG in lung cancer. J Nucl Med. 2009;50:1948–53. https://doi.org/10.2967/jnumed.109.069021.
53. Kositwattanarerk A, Oh M, Kudo T, Kiyono Y, Mori T, Kimura Y, et al. Different distribution of (62) Cu ATSM and (18)F-FDG in head and neck cancers. Clin Nucl Med. 2012;37:252–7. https://doi.org/10.1097/RLU.0b013e31823eaadb.
54. Ikawa M, Okazawa H, Arakawa K, Kudo T, Kimura H, Fujibayashi Y, et al. PET imaging of redox and energy states in stroke-like episodes of MELAS. Mitochondrion. 2009;9:144–8. https://doi.org/10.1016/j.mito.2009.01.011.
55. Ikawa M, Okazawa H, Kudo T, Kuriyama M, Fujibayashi Y, Yoneda M. Evaluation of striatal oxidative stress in patients with Parkinson's disease using [62Cu]ATSM PET. Nucl Med Biol. 2011;38:945–51. https://doi.org/10.1016/j.nucmedbio.2011.02.016.
56. Isozaki M, Kiyono Y, Arai Y, Kudo T, Mori T, Maruyama R, et al. Feasibility of 62Cu-ATSM PET for evaluation of brain ischaemia and misery perfusion in patients with cerebrovascular disease. Eur J Nucl Med Mol Imaging. 2011;38:1075–82. https://doi.org/10.1007/s00259-011-1734-z.
57. Tateishi K, Tateishi U, Sato M, Yamanaka S, Kanno H, Murata H, et al. Application of 62Cu-diacetyl-bis (N4-methylthiosemicarbazone) PET imaging to predict highly malignant tumor grades and hypoxia-inducible factor-1alpha expression in patients with glioma. AJNR Am J Neuroradiol. 2013;34:92–9. https://doi.org/10.3174/ajnr.A3159.
58. Dehdashti F, Mintun MA, Lewis JS, Bradley J, Govindan R, Laforest R, et al. In vivo assessment of tumor hypoxia in lung cancer with 60Cu-ATSM. Eur J Nucl Med Mol Imaging. 2003;30:844–50. https://doi.org/10.1007/s00259-003-1130-4.
59. Dehdashti F, Grigsby PW, Mintun MA, Lewis JS, Siegel BA, Welch MJ. Assessing tumor hypoxia in cervical cancer by positron emission tomography with 60Cu-ATSM: relationship to therapeutic response-a preliminary report. Int J Radiat Oncol Biol Phys. 2003;55:1233–8. https://doi.org/10.1016/s0360-3016(02)04477-2.
60. Lewis J, Laforest R, Buettner T, Song S, Fujibayashi Y, Connett J, et al. Copper-64-diacetyl-bis(N4-methylthiosemicarbazone): an agent for radiotherapy. Proc Natl Acad Sci U S A. 2001;98:1206–11. https://doi.org/10.1073/pnas.98.3.1206.
61. McMillan DD, Maeda J, Bell JJ, Genet MD, Phoonswadi G, Mann KA, et al. Validation of 64Cu-ATSM damaging DNA via high-LET Auger electron emission. J Radiat Res. 2015;56:784–91. https://doi.org/10.1093/jrr/rrv042.
62. Obata A, Yoshimoto M, Kasamatsu S, Naiki H, Takamatsu S, Kashikura K, et al. Intra-tumoral distribution of (64)Cu-ATSM: a comparison study with FDG. Nucl Med Biol. 2003;30:529–34. https://doi.org/10.1016/s0969-8051(03)00047-7.
63. Lewis JS, Laforest R, Dehdashti F, Grigsby PW, Welch MJ, Siegel BA. An imaging comparison of 64Cu-ATSM and 60Cu-ATSM in cancer of the uterine cervix. J Nucl Med. 2008;49:1177–82. https://doi.org/10.2967/jnumed.108.051326.
64. Savi A, Incerti E, Fallanca F, Bettinardi V, Rossetti F, Monterisi C, et al. First evaluation of PET-based human biodistribution and dosimetry of (18)F-FAZA, a tracer for imaging tumor hypoxia. J Nucl Med. 2017;58:1224–9. https://doi.org/10.2967/jnumed.113.122671.
65. Nakajo M, Jinguji M, Tani A, Kajiya Y, Nandate T, Kitazano I, et al. [(18)F]-FDG-PET/CT and [(18)F]-FAZA-PET/CT hypoxia imaging of metastatic thyroid cancer: association with short-term progression after radioiodine therapy. Mol Imaging Biol. 2020;22:1609–20. https://doi.org/10.1007/s11307-020-01516-6.
66. Little PV, Arnberg F, Jussing E, Lu L, Ingemann Jensen A, Mitsios N, et al. The cellular basis of increased PET hypoxia tracer uptake in focal cerebral ischemia with comparison between [(18)F]FMISO and [(64)Cu]CuATSM. J Cereb Blood Flow Metab. 2021;41:617–29. https://doi.org/10.1177/0271678X20923857.
67. Williamson DJ, Ejaz S, Sitnikov S, Fryer TD, Sawiak SJ, Burke P, et al. A comparison of four PET tracers for brain hypoxia mapping in a rodent model of stroke. Nucl Med Biol. 2013;40:338–44. https://doi.org/10.1016/j.nucmedbio.2012.11.012.
68. Takasawa M, Moustafa RR, Baron JC. Applications of nitroimidazole in vivo hypoxia imaging in ischemic stroke. Stroke. 2008;39:1629–37. https://doi.org/10.1161/STROKEAHA.107.485938.
69. Liu T, Redalen KR, Karlsen M. Development of an automated production process of [(64) Cu][Cu (ATSM)] for positron emission tomography imaging and theranostic applications. J Labelled Comp Radiopharm. 2022;65:191–202. https://doi.org/10.1002/jlcr.3973.
70. Laforest R, Dehdashti F, Lewis JS, Schwarz SW. Dosimetry of 60/61/62/64Cu-ATSM: a hypoxia imaging agent for PET. Eur J Nucl Med Mol Imaging. 2005;32:764–70. https://doi.org/10.1007/s00259-004-1756-x.
71. Yoshii Y, Matsumoto H, Yoshimoto M, Zhang MR, Oe Y, Kurihara H, et al. Multiple administrations of (64)Cu-ATSM as a novel therapeutic option for glioblastoma: a translational study using mice with xenografts. Transl Oncol. 2018;11:24–30. https://doi.org/10.1016/j.tranon.2017.10.006.
72. Yoshii Y, Matsumoto H, Yoshimoto M, Furukawa T, Morokoshi Y, Sogawa C, et al. Controlled administration of penicillamine reduces radiation exposure in critical organs during 64Cu-ATSM internal radiotherapy: a novel strategy for liver protection. PLoS ONE. 2014;9:e86996. https://doi.org/10.1371/journal.pone.0086996.
73. Igarashi C, Matsumoto H, Takahashi M, Hihara F, Tachibana T, Zhang MR, et al. Identification and quantitative structure-activity relationship assessment of trace chemical impurities contained in the therapeutic formulation of [(64)Cu]Cu-ATSM. Nucl Med Biol. 2022;108–109:10–5. https://doi.org/10.1016/j.nucmedbio.2022.02.001.
74. Liu T, Karlsen M, Karlberg AM, Redalen KR. Hypoxia imaging and theranostic potential of [(64)Cu][Cu(ATSM)] and ionic Cu(II) salts: a review of current evidence and discussion of the retention mechanisms. EJNMMI Res. 2020;10:33. https://doi.org/10.1186/s13550-020-00621-5.

75. Yoshii Y, Furukawa T, Kiyono Y, Watanabe R, Waki A, Mori T, et al. Copper-64-diacetyl-bis (N4-methylthiosemicarbazone) accumulates in rich regions of CD133+ highly tumorigenic cells in mouse colon carcinoma. Nucl Med Biol. 2010;37:395–404. https://doi.org/10.1016/j.nucmedbio.2009.12.011.
76. Yoshii Y, Furukawa T, Kiyono Y, Watanabe R, Mori T, Yoshii H, et al. Internal radiotherapy with copper-64-diacetyl-bis (N4-methylthiosemicarbazone) reduces CD133+ highly tumorigenic cells and metastatic ability of mouse colon carcinoma. Nucl Med Biol. 2011;38:151–7. https://doi.org/10.1016/j.nucmedbio.2010.08.009.
77. Wallace JL, Wang R. Hydrogen sulfide-based therapeutics: exploiting a unique but ubiquitous gasotransmitter. Nat Rev Drug Discov. 2015;14:329–45. https://doi.org/10.1038/nrd4433.
78. Pyun J, McInnes LE, Donnelly PS, Mawal C, Bush AI, Short JL, et al. Copper bis(thiosemicarbazone) complexes modulate P-glycoprotein expression and function in human brain microvascular endothelial cells. J Neurochem. 2022;(3):226-244. https://doi.org/10.1111/jnc.15609
79. Sarkar S, Ha YS, Soni N, An GI, Lee W, Kim MH, et al. Immobilization of the gas signaling molecule H2 S by radioisotopes: detection, quantification, and in vivo imaging. Angew Chem Int Ed Engl. 2016;55:9365–70. https://doi.org/10.1002/anie.201603813.
80. Cheng XT, Huang N, Sheng ZH. Programming axonal mitochondrial maintenance and bioenergetics in neurodegeneration and regeneration. Neuron. 2022;110(12):1899–1923.
81. Eldeeb MA, Thomas RA, Ragheb MA, Fallahi A, Fon EA. Mitochondrial quality control in health and in Parkinson's disease. Physiol Rev. 2022;102(4):1721–1755.
82. Cisneros J, Belton TB, Shum GC, Molakal CG, Wong YC. Mitochondria-lysosome contact site dynamics and misregulation in neurodegenerative diseases. Trends Neurosci. 2022;45:312–22. https://doi.org/10.1016/j.tins.2022.01.005.
83. Amorim JA, Coppotelli G, Rolo AP, Palmeira CM, Ross JM, Sinclair DA. Mitochondrial and metabolic dysfunction in ageing and age-related diseases. Nat Rev Endocrinol. 2022;18:243–58. https://doi.org/10.1038/s41574-021-00626-7.
84. Lewis JS, Herrero P, Sharp TL, Engelbach JA, Fujibayashi Y, Laforest R, et al. Delineation of hypoxia in canine myocardium using PET and copper(II)-diacetyl-bis(N(4)-methylthiosemicarbazone). J Nucl Med. 2002;43:1557–69.
85. Nie X, Elvington A, Laforest R, Zheng J, Voller TF, Zayed MA, et al. (64)Cu-ATSM positron emission tomography/magnetic resonance imaging of hypoxia in human atherosclerosis. Circ Cardiovasc Imaging. 2020;13:e009791. https://doi.org/10.1161/CIRCIMAGING.119.009791.